Late Blight Detection in Tomato Fields by Aerial Photography with Natural and Infrared Color Film

C. H. BLAZQUEZ, University of Florida, Institute of Food and Agricultural Sciences, Citrus Research and Education Center, Lake Alfred 33850

ABSTRACT

Blazquez, C. H. 1990. Late blight detection in tomato fields by aerial photography with natural and infrared color film. Plant Dis. 74:589-592.

Natural color and infrared color aerial photographs of tomato (*Lycopersicon esculentum*) canopies were taken weekly with paired 35-mm cameras during the 1976 spring growing season. Loci of tomato late blight infections (caused by *Phytophthora infestans*) confirmed by field surveillance were drawn on field maps and compared with results of photographic analysis. Spectral densitometric measurements made on films from 400 to 700 nm in increments of 10 nm showed two intensity peaks with both types of film. Dividing the first peak by the second peak produced a ratio greater than 1 that correlated significantly with integral and transmittance measurements of color infrared photographs of diseased plants. Spectrophotometric measurements of color infrared photographs detected late blight on tomato plants better than visual observation of photographs.

Tomato (*Lycopersicon esculentum* Mill.) production in Lee, Hendry, and Collier counties in southwest Florida represents a sizable share of total vegetable production in the state. The resale value of Florida tomato products in 1986–1987 exceeded $515 million (11).

Late blight of tomato, caused by *Phytophthora infestans* (Mont.) de Bary, is a foliar disease that can cause severe damage in some plantings. Although the BLITECAST disease forecasting system (7,9) can be used under Florida conditions to schedule fungicide applications, fields are scouted periodically to detect the presence and severity of disease. This technique of crop evaluation is tedious, time-consuming, and costly and requires keeping records of areas prone to disease.

Aerial photography with 35-mm color infrared (CIR) film (Kodak 2443 Aerochrome) has been used to detect vegetable diseases (1,2), study rangeland vegetation from fixed-wing aircraft (10,12,13), and observe environmental stress (6). This type of infrared film (Kodak 2443) was developed in the 1960s (12) and has continued to be used for aerial photography over the years. More recently, aerial photography with 35-mm CIR film has been used to study the tomato-producing area near Homestead, FL (Paul Orth, *personal communication*) and potato fields in Aroostook County, ME (Frank Manzer, *personal communication*), as a surveillance tool for detecting initial outbreaks of late blight, and to monitor field control of late blight.

Exploratory experiments were conducted from January through May 1976 (C. H. Blazquez, *unpublished*) in southwest Florida to determine whether aerial CIR photographic surveys could detect late blight of tomato and monitor its spread throughout a growing season. The results were positive but were not critically evaluated at that time, because neither sensitive densitometers nor radiometers (8) were available to discern differences between healthy and diseased tomato canopies. Recent developments of an image analysis system, scanning densitometer, and interactive computer program (3,4) have made it possible to analyze the 1976 photographs with greater accuracy.

The objectives of this study were to critically evaluate aerial surveillance photographs, to demonstrate the value of combining a scanning densitometer and an interactive computer program for analyzing spectral data, and to compare the use of natural color (NC) and CIR film in detecting tomato late blight epidemics.

MATERIALS AND METHODS

Field surveillance. Three fields (A, B, and C) were selected within 30-min flying distance of the airport used as a base of operations. Arrangements were made with cooperating growers for marking unstaked tomato beds (rows) planted with cultivar Walter tomatoes. Fields varied in size from 60.7 ha (150 acres) to 101.5 ha (250 acres).

Fields were visited after the aerial photographs were visually interpreted. Because the pathogen spreads rapidly, ground surveillance (scouting) was completed within 12 hr of the photographic mission. Field visits concentrated on areas suspected of being disease loci. Disease areas noted in aerial photographs were divided into three transects, one through the center of the disease area and the other two covering the outer perimeters. The percentage of disease was estimated by the method of Brown, Barratt, and Horsfall (5). Scouts made 10 stops along each transect, estimated the percentage of diseased plants among all plants within a 2-m radius of each stop, and averaged the results from the three transects to assign visual grades of late blight damage.

Aerial field photographs. Aerial photographs of tomato fields with naturally occurring late blight were taken from varying altitudes (121, 152, and 305 m) with hand-held paired Pentax Spotmatic

Florida Agricultural Experiment Station Journal Series No. 9591.

Accepted for publication 22 January 1990 (submitted for electronic processing).

Table 1. Tomato late blight severity (%) visually interpreted from 35-mm natural color (NC) and color infrared (CIR) aerial photographs and estimated by ground surveillance (GR) of three fields during the 1976 growing season

Flight date		Field A			Field B			Field C		
		NC	GR	CIR	NC	GR	CIR	NC	GR	CIR
January	3	0	0	0	0	0	0	0	0	0
	9	5	5	10	10	10	10	0	5	5
	16	10	10	15	15	15	15	10	10	15
	23	15	15	20	15	15	15	15	15	15
	30	15	20	20	15	15	20	15	15	15
February	7	10	10	10	15	15	15	10	10	15
	14	10	10	10	15	15	15	10	10	10
	21	5	5	5	10	10	10	10	5	5
	28	5	5	10	10	5	5	10	5	5
March	4	15	10	15	15	10	10	15	15	20
	11	15	10	15	10	5	5	10	5	5
	18	20	15	25	15	10	10	10	5	5
	25	15	10	25	20	10	10	15	10	10
April	1	15	15	30	20	10	10	15	15	15
	8	10	15	20	25	15	20	15	15	20
	15	10	10	15	20	15	20	10	10	10
	22	10	10	15	10	5	5	10	10	10
	29	10	10	10	10	10	10	10	10	10
May	6	5	5	10	10	5	5	10	10	10
	13	5	5	5	5	5	5	5	5	10
	20	5	5	10	5	5	5	5	5	5
	27	5	2	5	5	2	2	5	5	5
r[a]		0.73		0.81	0.78		0.95	0.84		0.95

[a] Linear correlation coefficient. Correlation coefficients were significant at the 5% level at 0.42 and at the 1% level at 0.54 for all columns.

cameras with 135-mm, f2.8 telephoto lenses. Lens apertures varied from f/4.0 to f/8.0 with Ektachrome NC film. Kodak Aerochrome 2443 CIR film was exposed at f/5.6 with a No. 12 yellow Wratten filter. Shutter speeds were 0.004 sec for NC film and 0.002 sec for CIR film. Twelve photographs were taken per field per mission with each type of film, for a total of 1,584 photographs completed during the project.

Aerial photographs were interpreted through a stereomicroscope at a magnification of ×80 and were compared with close-up photographs of diseased tomato plants. Sketch maps of each photographic flight were prepared with infection sites marked as polygons and were recorded on plastic overlays of the planted areas to chart disease progress. No efforts were made to associate disease surveillance with ground control of the disease. In all, 22 overflights were made between planting time and the first harvest (Table 1).

Densitometry. A halogen bulb was used as a light source in a microfiche reader (Jenoptik Jena GmbH Dokumator DL-2) with magnifications of ×6.5, 9.0, 13.0, and 17.5. The projection screen was replaced with an aluminum

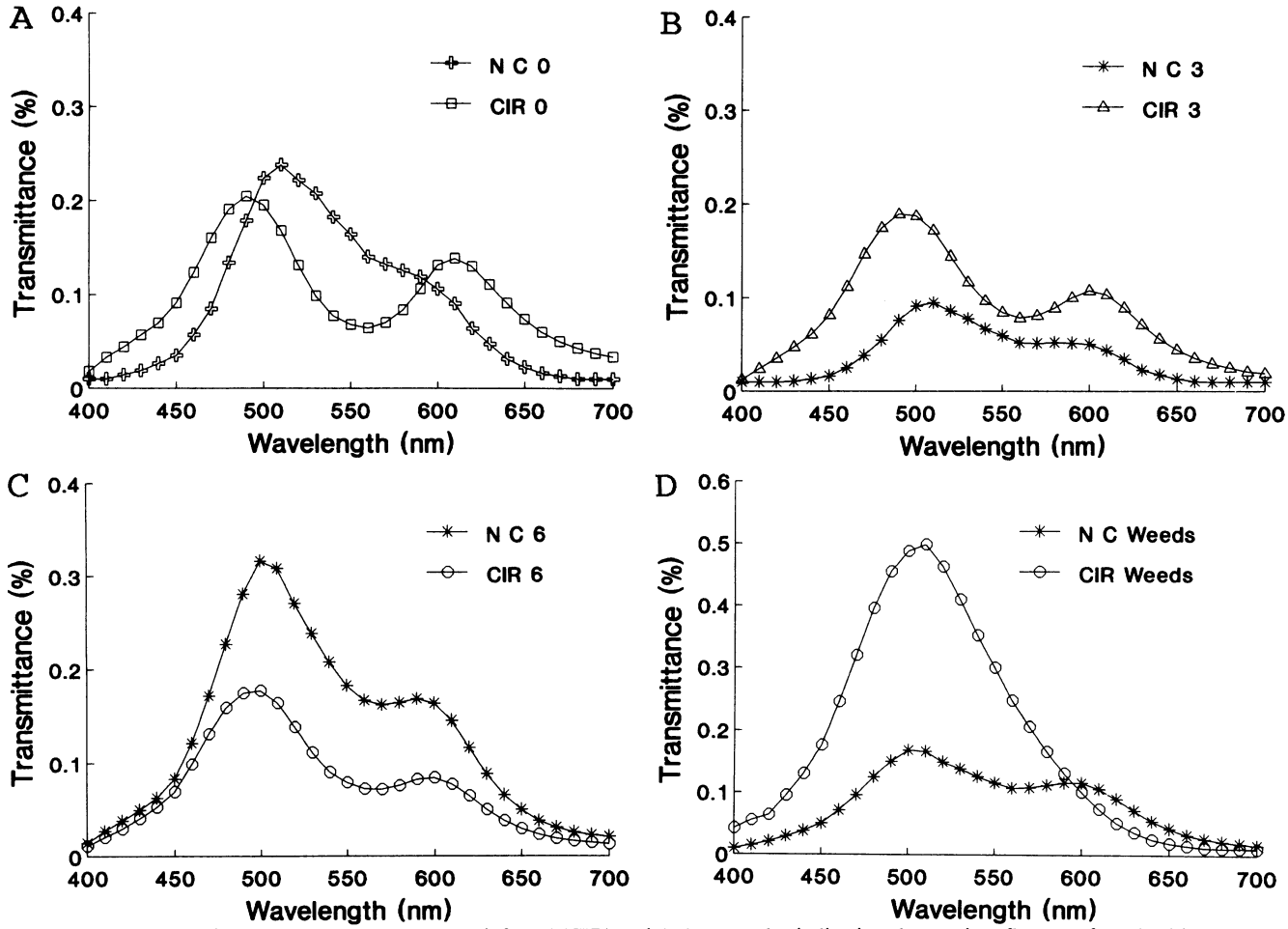

Fig. 1. Spectral curves of natural color (NC) and color infrared (CIR) aerial photographs, indicating changes in reflectance from healthy tomatoes **(A)** (level 0 = 1.17% of plants diseased), tomatoes with late blight disease (caused by *Phytophthora infestans*) at severity level 3 (9.37% of plants infected) **(B)** and level 6 (62.5% infection) **(C)**, and weed reflectance **(D)**. Two peaks were found, at the 480–490 nm and the 610–620 nm wavelengths of healthy tomatoes, whereas only one peak was found in the CIR curve of weeds.

plate covered with white poster board. A Gamma Scientific flexible fiber-optic probe (914 × 3.18 mm) was installed near the center of the plate. The face of the probe was held flush with the face of the screen by a brass plate on the underside of the aluminum plate. The other end of the fiber-optic probe was connected to a monochromator (model 700-3, Gamma Scientific Inc., San Diego, CA) containing Bausch & Lomb visible grating (cat. no. 33-86, 1976). Light from the monochromator was measured through a Gamma Scientific exit C type slit (0.75 mm) mounted in front of an R-777 Hamamatsu photomultiplier. The resulting output was read on a photovoltmultiplier-photometer (model 250-A, Photovolt Corp., New York, NY).

Spectral analysis of each site was done by positioning the transparency over the aperture. The monochromator was manually scanned in increments of 10 nm from 400 to 700 nm. Five light transmittance values displayed in the photometer from each wavelength of the photographed site were manually entered into a computer program, for a total of 155 densitometric readings. The program also measured the transmittance of each curve and summarized the data entered.

The spectral data were analyzed by dividing the two maximum transmittance peaks to determine a transmittance ratio (SRT), as indicated by the following formulas: integral 1 divided by integral 2 (I1/I2) = spectral integral ratio (SRG), where integral 1 is the first peak in the spectral curve (480–490 nm) and integral 2 is the second peak (610–620 nm); and transmittance 1 divided by transmittance 2 (T1/T2) = spectral transmittance ratio (SRT), where T1 is the maximum transmittance (first peak) in the spectral curve (480–490 nm) and T2 is the maximum transmittance (second peak) at 610–620 nm.

Transparencies for densitometric measurements were selected from photographic missions where healthy and late blight-diseased foliage had been detected at sufficient levels of severity. Rows measured were representative of three visual ratings of disease: 0, 3, and 6 on a scale from 0 to 10, where a rating of 0 = 1.17% and 10 = 97.66% (5).

RESULTS AND DISCUSSION

Weekly aerial photographic surveillance of the three test fields over a period of 22 wk indicated that it was possible to observe low levels of tomato late blight and to detect its incidence at high levels of infection (Table 1). Sketch maps were prepared by projecting aerial photographs (at the same scale as maps of planted fields) on a screen covered with transparent mylar film. Diseased areas were marked on the mylar for future comparisons. Verification of the photointerpreted data and sequential field observations required additional time not anticipated in the design of the experiment.

Interpretation of the NC film transparencies was more difficult than interpretation of the CIR film because disease damage was less evident; however, once disease areas were observed in the CIR film, they could also be detected in the NC film. Field estimation of disease was more reliable than photography at the beginning of the project, but confidence in photointerpretation grew with experience and verification. Use of a spectral densitometer (4) and an interactive computer program made it possible to compare the usefulness of NC and CIR films for detecting tomato late blight and correlated well with visual observations.

Densitometric measurements yielded two peak transmittances at 510 nm (T1) and 610 nm (T2) for NC film and 490 nm (T1) and 610 nm (T2) for CIR film. Densitometric measurements of NC transparencies of healthy and diseased rows indicated that the shapes of the NC transmittance curves were similar for 0, 3, and 6% late blight severity grades (Fig. 1A–C), whereas the curve for percentage transmittance of weeds (Fig. 1D) differed from those of tomato. The integral (the measured area under a curve) values (I1 and I2) of the NC curves correlated well ($P = 0.01$) with the visual observations ($r = 0.79$ and 0.78, respectively). However, the ratio I1/I2 of the two was not significant ($r = 0.3$; $P > 0.05$) (Table 2). The results were similar to the transmittance values (T1 and T2), where individual transmittances (0.7 and 0.81) were highly significant ($P = 0.01$) (1%), but their ratio was not (−0.23; $P > 0.05$).

The shape of the CIR curves of visual severity values 0 and 3 did not vary greatly, but a slight drop in the percentage transmittance at 600 nm was detected for visual severity value 6, with no second peak at all in the weed curve (Fig. 1D). The integral values of the CIR curves of the same rows indicated that the curves for severity values 0 and 3 (Fig. 1A,B) were very similar, but transmittance dropped at the 600-nm wavelength detectable at visual severity value 6 (Fig. 1C).

Densitometric measurements indicated that the spectral curves of NC film did not clearly detect levels of late blight. Integral measurements of the two peaks were significantly correlated with visual observations, whereas the ratio of the two NC film integrals was not significant (Table 2). Correlation was obtained with the transmittances T1 and T2, but their ratio was not significant (Table 2).

Densitometric measurements of CIR photographs produced different results. The spectral curves of healthy rows did not differ greatly from those of visual severity rank 3, but a slight drop in transmittance was detected in the curve of visual severity rank 6, and the curve from rows with weeds only had no second peak (Table 3). Analysis of the CIR integrals indicated that I1 was not significant and did not correlate well with visual observations. However, both I2 and the ratio (SRT) were significantly correlated with field observations. CIR T1 and T2 were negatively correlated with visual rankings; their ratio, however, had a higher positive correlation than the NC ratio of transmittance.

Table 2. Visual field observations of tomato late blight disease severity[a] and densitometric measurements[b] from natural color photographs of healthy and diseased rows of tomatoes

	Natural color photographs[b]					
Field rank[a]	I1	I2	SRG ratio	T1 (%)	T2 (%)	SRT ratio
0	8.07	3.55	2.19	0.09	0.06	1.82
0	11.72	5.35	2.19	0.13	0.08	1.63
0	11.62	5.33	2.18	0.13	0.08	1.63
0	11.70	5.35	2.19	0.17	0.09	1.44
0	8.07	3.35	2.27	0.09	0.12	1.82
0	11.71	5.31	2.21	0.13	0.08	1.63
0	10.71	5.30	2.15	0.13	0.08	1.63
0	8.10	3.52	2.26	0.09	0.05	1.72
3	13.78	6.65	2.07	0.15	0.09	1.59
3	13.75	6.64	2.07	0.15	0.12	1.59
3	13.77	6.62	2.07	0.15	0.12	1.59
6	28.32	11.63	2.43	0.32	0.17	1.89
6	17.83	7.25	2.46	0.20	0.11	1.85
6	28.13	11.50	2.42	0.31	0.17	1.84
6	17.80	7.21	2.45	0.19	0.11	1.84
6	25.02	10.61	2.31	0.31	0.17	1.89
Weeds	15.15	9.77	1.55	0.17	0.12	1.44
Soil	30.56	17.13	1.78	0.29	0.22	1.30
r[c]	0.79	0.79	0.31	0.74	0.81	−0.23

[a] Rows were ranked for percentage of diseased plants by visual observations from 1 through 10 (where 1 = 1.17% and 10 = 97.66%).

[b] Intensity (%) of transmittances (T1 and T2), integrals of curves (I1 and I2), spectral integral ratios (SRG) = I2/I1, and spectral transmittance ratios (SRT) = T2/T1.

[c] Linear correlation coefficient. Correlation coefficients were significant at the 5% level at 0.47 and at the 1% level at 0.59 for all columns.

Table 3. Visual field observations of tomato late blight disease severity[a] and densitometric measurements[b] from aerial color infrared (Aerochrome 2443) photographs of healthy and diseased rows of tomatoes

Field rank[a]	Infrared color photographs[b]					
	I1	I2	SRG ratio	T1 (%)	T2 (%)	SRT ratio
0	19.16	11.51	1.67	0.22	0.14	1.63
0	17.49	11.69	1.47	0.20	0.14	1.48
0	17.16	8.66	1.90	0.19	0.11	2.11
0	17.49	11.69	1.47	0.20	0.14	2.11
0	19.15	11.55	1.65	0.22	0.14	1.63
0	17.32	11.65	1.49	0.20	0.14	1.47
0	17.59	11.79	1.50	0.21	0.14	1.48
3	8.97	8.97	1.91	0.19	0.11	1.76
3	17.16	8.88	1.91	0.19	0.11	1.76
6	19.22	6.73	2.89	0.20	0.09	2.18
6	16.43	6.16	2.67	0.18	0.08	2.10
6	18.11	6.75	2.75	0.20	0.09	2.15
6	16.50	6.14	2.66	0.18	0.08	2.10
6	17.16	8.66	1.90	0.19	0.11	2.10
6	16.44	6.17	2.67	0.18	0.09	2.10
6	17.46	6.18	2.65	0.18	0.08	2.11
Weeds	39.89	—	—	—	—	0.50
Soil	62.61	—	—	0.77	—	—
r[c]	−0.40	−0.51	0.78	−0.75	−0.99	0.95

[a] Rows were ranked for percentage of diseased plants by visual observations from 1 through 10 (where 1 = 1.17% and 10 = 97.66%).
[b] Intensity (%) of transmittances (T1 and T2), integrals of curves (I1 and I2), spectral integral ratios (SRG = I1/I2), and spectral transmittance ratios (SRT = T1/T2).
[c] Linear correlation coefficient. Correlation coefficients were significant at the 5% level at 0.47 and at the 1% level at 0.59 for all columns.

Results of experiments with tomato fields indicated that aerial photography provided a synoptic overview of entire fields and made it possible to observe at one time the most productive areas as well as those with disease problems. Photography with both types of film provided a permanent record of observations for subsequent interpretation. CIR photography yielded greater contrast between healthy and diseased tomato plants than NC film, making it easier to detect areas of potential problems. The use of sketch mapping and overlays helped to monitor late blight occurrence throughout the growing season.

Although CIR film is not easy to handle and requires refrigeration before and after exposure until developed (9), its advantages outweigh these problems. In NC film, the contrast is between green and brown, whereas for CIR, it is between magenta (reddish pink) and cyan (light blue); thus, the differences are more accentuated with CIR than with NC film in most photographs. Results of visual interpretations were less conclusive (Table 1) than those obtained with densitometry (Tables 2 and 3), where the differences between the two types of film were more clearly defined.

LITERATURE CITED

1. Blazquez, C. H. 1973. Detection of foliar diseases of vegetable crops with color infrared photography. Am. Soc. Photogramm. Color Workshop 3:236-244.
2. Blazquez, C. H., and Edwards, G. J. 1983. Infrared color photography and spectral reflectance of tomato and potato diseases. J. Appl. Photogr. Eng. 9:33-37.
3. Blazquez, C. H., and Edwards, G. J. 1985. Image analysis of tomato leaves with late blight. J. Imaging Technol. 11:109-112.
4. Blazquez, C. H., Richardson, A. J., Nixon, P. R., and Escobar, D. 1988. Densitometric measurements and image analysis of aerial color infrared photographs. J. Imaging Technol. 14:37-42.
5. Brown, I. F., Barratt, R. W., and Horsfall, J. W. 1968. Elanco conversion table for Barratt-Horsfall rating system. Special Report, Eli Lilly & Co., Greenfield, IN. 110 pp.
6. Clegg, R. H., and Scherz, J. P. 1975. A comparison of 9-inch, 70 mm and 35 mm cameras. Photogramm. Eng. Remote Sens. 41:1487-1500.
7. Krause, R. A., and Massie, L. B. 1975. Predictive systems: Modern approaches to disease control. Annu. Rev. Phytopathol. 13:31-47.
8. Lathrop, L. P., and Pennypacker, S. P. 1980. Spectral classification of tomato disease severity levels. Photogramm. Eng. Remote Sens. 46:1433-1438.
9. MacKenzie, D. R. 1981. Scheduling fungicide applications for potato late blight with BLITECAST. Plant Dis. 65:394-399.
10. Meyer, M. B., Eng, R., and Gjersing, F. 1973. A 35 mm aerial photographic system for forest and range resource analysis. Minn. Coll. For. Res. Note 240. 4 pp.
11. Taylor, T. D., and Smith, S. A. 1988. Production of selected Florida vegetables 1987-1988. Economics Information Report 245. Food and Resource Economics Department, Institute of Food and Agricultural Sciences, University of Florida. 51 pp.
12. Tueller, P. T., Lent, P. C., Stager, R. D., Jacobsen, E. A., and Platou, K. A. 1988. Rangeland vegetation changes measured from helicopter-borne 35 mm aerial photography. Photogramm. Eng. Remote Sens. 54:609-614.
13. Waller, S. S., Lewis, J. K., Brown, M. A., Heintz, T. W., Butterfield, R. I., and Gartner, F. R. 1978. Use of 35 mm aerial photography in vegetation sampling. Pages 517-520 in: Proc. Int. Range Congr. 1st, Denver, CO. Range Management Association.